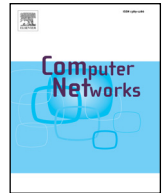




Contents lists available at ScienceDirect

## Computer Networks

journal homepage: [www.elsevier.com/locate/comnet](http://www.elsevier.com/locate/comnet)

## Performance analysis of prioritized broadcast service in WAVE/IEEE 802.11p

Peng Zhou<sup>a,b</sup>, Yanheng Liu<sup>a,b,c</sup>, Jian Wang<sup>a,b,c,d,\*</sup>, Weiwen Deng<sup>c</sup>, Heekuck Oh<sup>d</sup>

<sup>a</sup> College of Computer Science and Technology, Jilin University, Changchun 130012, China

<sup>b</sup> Key Laboratory of Symbolic Communication and Knowledge Engineering of Ministry of Education, Jilin University, Changchun 130012, China

<sup>c</sup> State Key Laboratory of Automotive Simulation and Control, Jilin University, Changchun 130012, China

<sup>d</sup> Department of Computer Science and Engineering, Hanyang University, Ansan 426791, South Korea

## ARTICLE INFO

## Article history:

Received 4 September 2015

Revised 12 April 2016

Accepted 13 April 2016

Available online xxx

## Keywords:

WAVE

IEEE 802.11p

EDCA

Performance analysis

Markov model

## ABSTRACT

In this paper, we propose a more accurate model to capture the prioritized broadcast service in WAVE/IEEE 802.11p and comprehensively analyze the related performance indicators accordingly. We construct a 2-D Markov chain to characterize the IEEE 802.11p EDCA backoff process and subsequently build a 1-D infinite discrete-time Markov chain to identify the contention period for establishing the relation between the transmission probabilities and the channel state. We also consider the impacts of the multichannel operation defined by IEEE 1609.4 in the modeling. Unlike most previous work, we define the transmission probability as a function of the fluctuating numbers of continuous idle slots, introduce a proactive backoff stage into the 2-D Markov chain to profile the backoff procedure where the transmission queue is empty, and characterize the access delay extension and transmission synchronization caused by channel switching. We perform extensive numerical analyses and investigate the access delay, packet delivery rate, and other performance indicators. The results uncover the relations among the metrics of concern underlying various priority access categories as a function of the experienced traffic loads. The effectiveness of the proposed performance model is faithfully verified by the simulation results.

© 2016 Elsevier B.V. All rights reserved.

### 1. Introduction

It is envisioned that the deployment of Information and Communication Technologies (ICTs) in modern Intelligent Transportation Systems (ITS) will contribute to great improvements in the quality, effectiveness, and safety of future transportation systems. As one of the candidate network architectures, Vehicular Ad-hoc Networks (VANETs) are a special type of mobile ad-hoc network created by moving cars and roadside units in a self-organized manner without any permanent infrastructure. Owing to their decentralized nature, VANETs are highly preferred by a variety of safety applications that cannot easily obtain help from central nodes—e.g., cooperative collision avoidance, blind spot warning, and approaching emergency warning. However, the significant characteristics of VANETs (e.g., frequently changed topology, worse signal to noise ratio, and non-ignorable Doppler effect) introduce new nontrivial challenges in designing communication protocols as well.

To address these issues, the Wireless Access in Vehicular Environments (WAVE) standard has been proposed by IEEE, which is composed of the IEEE 802.11p MAC/PHY protocol, together with the IEEE 1609 protocol family (denoted by IEEE 1609.x) as the higher-layer standard to serve ITS applications in multichannel operation, networking service, and security. In particular, the WAVE standard amends and extends the IEEE 802.11 standard at the PHY and MAC layers. At the PHY layer, IEEE 802.11p works on several channels within the frequency band spanning the 5.9 GHz (5.85–5.925 GHz) range dedicated to ITS known as the DSRC (Dedicated Short-Range Communications) band. One of them, known as the Control Channel (CCH), is used exclusively for the dissemination of safety- and management-related messages, and the remaining six are marked as the Service Channel (SCH) for various applications (e.g., infotainment) data. At the MAC layer, IEEE 802.11p is derived from the IEEE 802.11e enhanced distributed channel access (EDCA) function by excluding the multiple-frame transmission [Transmission Opportunity (TXOP)] feature and simplifies the authentication and association operations, which are considered to be time-consuming for vehicular communications. In terms of the priorities of the served traffic flows, IEEE 802.11p sorts the packets into a transmission queue associated with one of four access categories (ACs, the lowest priority corresponds to AC<sub>0</sub> and the

\* Corresponding author at: NO.2699 Qianjin Avenue, Changchun 130012, China. Tel.: +86 431 8516 8355; fax: +86 431 8516 8377.

E-mail address: [wangjian591@jlu.edu.cn](mailto:wangjian591@jlu.edu.cn) (J. Wang).

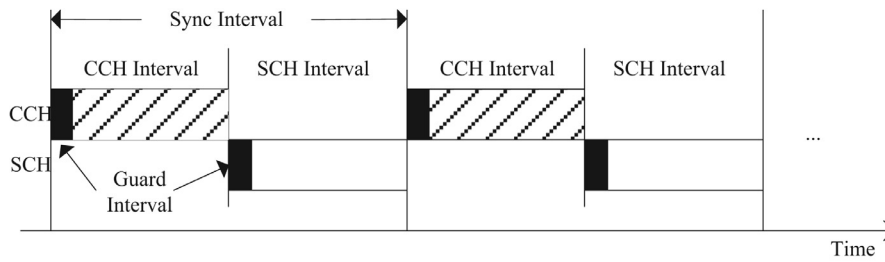


Fig. 1. CCH/SCH timing.

Table 1 Default EDCA parameter values in the IEEE 802.11p.

AC	CWmin	CWmax	AIFSN
AC <sub>0</sub>	aCWmin	aCWmax	9
AC <sub>1</sub>	aCWmin	aCWmax	6
AC <sub>2</sub>	(aCWmin+1)/2-1	aCWmin	3
AC <sub>3</sub>	(aCWmin+1)/4-1	(aCWmin+1)/2-1	2

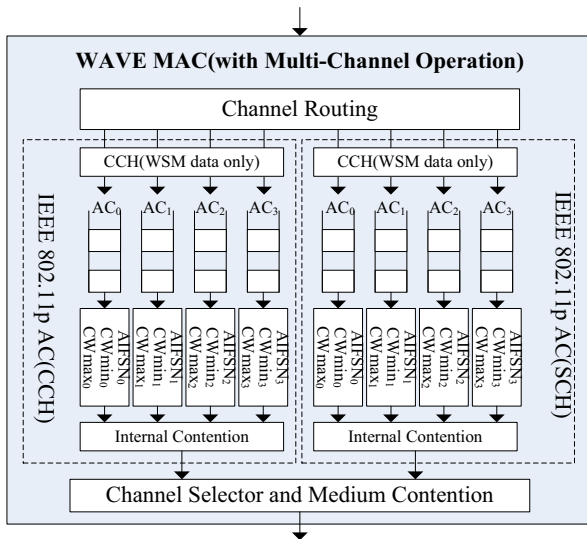


Fig. 2. Channel coordination in IEEE 1609.4.

highest to AC<sub>3</sub> in this paper) with different parameters to contend for access to the channel (involving the internal and external contentions). Table 1 shows the default EDCA parameter values in the standard [1] (aCWmin and aCWmax are generally set to 15 and 1023, respectively). In addition, IEEE 1609.4 specifies multichannel operations on top of IEEE 802.11p. Fig. 1 gives the alternative access scheme [2] that is the default access mode in IEEE 1609.4. All nodes synchronously tune to the CCH or switch to one of the SCHs every 50 ms. As a general rule, a station should equip several separate IEEE 802.11p MAC entities for CCH and SCH, as shown in Fig. 2 [2]. Thus, the performance can be effectively improved on the premise that all safety-related information can be detected.

However, because of the aforementioned amendments, it is necessary to build a different MAC model from the previous IEEE 802.11 model to reevaluate the performance of the WAVE vehicular network, especially for the broadcast service that is extensively adopted by the majority of vehicular applications. In contrast to unicast, the broadcast data are transmitted without sending any control frames such as the RTS/CTS handshake and thus have no MAC-level acknowledgement (ACK) or retransmission. Given the massive reduction in access and transmission delays, two points should be noted on modeling the broadcast service of WAVE/IEEE

802.11p. (i) The stations remain idle and have no packets to send in their AC queues most of the time, so the MAC model should accommodate both the unsaturated and saturated conditions. (ii) In EDCA, the backoff counter is still decremented even if no packets wait in the queue when the channel is sensed to be idle, which is often neglected in most unicast models but should not be overlooked in the broadcast model. (iii) Most importantly, the size of the contention window is doubled by the internal collision rather than by the external collision in the broadcast. Thus, the assumption that the probability of a station transmitting in an arbitrary slot is constant and independent of the backoff procedure is inapplicable to the vehicular broadcast service but is commonly assumed in modeling the unicast service. For example, when AC<sub>0</sub> obtains a chance to access the channel—i.e., the idle time interval of channel is more than 9 time slots—this implies that the backoff procedure of AC<sub>3</sub> is obviously finished because its maximal contention window has a size of four. Apparently, AC<sub>3</sub> can access the channel with a smaller possibility (i.e., the arrival probability of a new packet) at this point than at the first few slots within the backoff process. (iv) Owing to the absence of retransmission, the packet loss ratio and throughput are affected significantly by the non-constant access and collision probability. (v) Channel switching results in the extension of access delay and the synchronization of transmission. ACs must suspend the backoff process when the nodes tune to an unusable channel, so the packets arriving at different instants within an unusable channel interval may be transmitted synchronously at the beginning of the next usable channel interval.

Regarding the above shortcomings, we propose a more accurate analytical model for the WAVE/IEEE 802.11p broadcast service by introducing the impacts of IEEE 1609.4 multichannel operation, the M/G/1 queue model for unifying the unsaturated and saturated conditions, and the Markov model with the non-constant and conditional transmission probability for the IEEE 802.11p EDCA mechanism. We perform extensive numerical analysis and investigate the access delay, packet delivery rate, and other performance indicators, and the results uncover the relations among the metrics of concern underlying various priority access categories against the experienced traffic loads. The effectiveness of the proposed performance model is faithfully verified by the simulation results. To the best of our knowledge, this is the first attempt to involve such complete factors in modeling the WAVE MAC sublayer.

The rest of this paper is organized as follows. Section 2 overviews the related work concerning the IEEE 802.11p performance study. Section 3 introduces the analytical model in detail followed by the extensive analytical results and simulation results in Section 4. Finally, Section 5 presents the study's conclusions and suggests future research.

2. Related work

There is some published research considering analytical models for the broadcast service in vehicular networks [3–7]. Gallardo

et al. [3] analyzed the performance of EDCA broadcast under the specific conditions of the CCH with different Markov chains for each AC, which is suitable for the non-saturated conditions in which traffic is assumed to be generated in a burst following a Poisson process, and the size of each burst obeys an exponential distribution. Hafeez et al. [4] presented an analytical model for the performance of broadcast services in the DSRC protocol, which is composed of two Markov chains to derive the probabilities of transmitting states but ignores the internal contention. Woo et al. [5] proposed the Markov model for broadcasting priority messages based on IEEE 802.11p, however, similar to [4], the messages are also classified into two different priorities (i.e., safety and non-safety) without internal contention, which is not in accordance to the standard. Ping et al. [6] modified the default parameters of the standard to ensure the absolute advantage of high priorities and analyzed the performance of broadcast service in the EDCA mechanism with strict priorities. Harry et al. [7] developed an IEEE 802.11p contention model coupled with traffic models to study the broadcasting performance in a practical vehicle distribution. In addition, there is also some other work [8–12] on the performance analysis of the IEEE 802.11p EDCA unicast; however, it is not directly applicable to the broadcast service.

A few analytical IEEE 802.11p models [12–14] have been proposed to account for WAVE channel switching. Masic et al. [12] proposed a recursive method to assess the basic access mode of channel switching operation for analyzing the unicast performance of the WAVE/IEEE 802.11p. Campolo et al. [13] computed the useful duration of a CCH interval and derived the packet delivery probability of a vehicle detecting an unpredictable hazard and broadcasting the alert in the one-hop neighborhood. Yin et al. [14] constructed an analytical model using a semi-Markov process in which the impacts of the multichannel operations are incorporated to evaluate MAC-level performance and reliability of safety message dissemination; however, the internal contention remains a severe problem. In addition, none of these models [12–14] consider the impact of transmission synchronization caused by channel switching.

The impacts of the backoff in the idle state are discussed in [12] and [15]. However, the work in [12] focused on the IEEE 802.11p unicast service, and the model in [15] was proposed for assessing the IEEE 802.11 distributed coordination function (DCF) without prioritization being available. In addition, all of these models are based on the assumption that the transmission probability of an AC queue is a constant, which restricts the investigation of the WAVE broadcast. Campolo et al. [16] formalized the transmission probability of successive  $n$  empty slots prior to the first transmission attempt; however, it is suitable only for the case in which all packets synchronously launch contention exactly at the beginning of the CCH interval and their lifetime is bounded to one CCH interval.

Our main contribution to the literature can be summarized as follows: (i) We construct a 2-D Markov chain to characterize the IEEE 802.11p EDCA backoff process, which considers all major factors that could affect the performance, including four access categories, the saturation condition, standard parameters, backoff in empty queue, backoff counter freeze, and internal collision. (ii) We consider the transmission probability as a variable against the fluctuated numbers of successive idle slots and build a 1-D infinite Markov chain to capture the relation between the transmission probabilities and the channel state. Using the 1-D chain, we can successively formulize the probability that the channel experiences the  $k$ th continuous idle slot and the transmission probability at the  $k$ th continuous idle slot. Additionally, merging the 2-D and 1-D Markov chains to a 3D Markov chain undoubtedly makes the model too complicated to be solved. This finding explains why we abandoned using the 3D Markov chain, which is proved to be

more accurate in modeling unicast. (iii) We quantitatively present the impacts of the channel operation on the performance, including the extension on the access delay caused by channel switching, and the effect of transmission synchronization on the packet delivery rate.

### 3. Analytical model

Several assumptions are made to produce a simplified yet high-fidelity analytic model. (i) Based on the definition of the default multichannel operation mode in the IEEE 1609.4 standard, each node is considered as an independent single-radio WAVE device operating in an alternative-switching mode with two IEEE 802.11p MAC entities for CCH and SCH. (ii) To make the model behave more realistically, we assume that each node transmits frames with traffic category  $AC_m$ ,  $m=0, 1, 2, 3$ , which arrives at the MAC layer following a Poisson distribution with average rate  $\lambda_m$ . (iii) We also assume that the channel is ideal—i.e., the packet losses due to the channel errors are excluded—which aims to simplify the model but without losing generality in the performance analysis of the MAC sublayer. In addition, the time unit is one physical slot—i.e., the fixed time interval specified in the IEEE 802.11p standard. To avoid ambiguity, the varying time interval between two consecutive decrements of the backoff counter is called the backoff slot.

#### 3.1. Backoff procedure

The EDCA mechanism is a channel access mechanism specially designed for supporting different QoS requirements at the MAC layer. It defines four ACs—i.e.,  $AC_3$ ,  $AC_2$ ,  $AC_1$ , and  $AC_0$  in a descending order. As shown in Fig. 2, each AC has a queue independently contending for transmission driven by its own parameters—e.g., *Minimum Contention Window* ( $CW_{min}$ ), *Maximum Contention Window* ( $CW_{max}$ ), and *Arbitration Inter-Frame Space Number* ( $AIFSN$ ). Concretely speaking, an AC with a small  $AIFSN$  and short contention window size has a high priority to access the channel.

After finishing the preceding transmission of  $AC_m$ , the station restarts the backoff counter for  $AC_m$  with a random initial value from 0 to  $CW_{min_m}$ . During the backoff period, if the channel is busy, the backoff counter is frozen at the current value until the channel stays idle again for a duration  $AIFS_m = SIFS + AIFSN_m \cdot \sigma$ , where  $\sigma$  is the duration of a physical slot time, and  $SIFS$  is the duration of a *short inter-frame space*. The expression  $AIFS_m$  in units of slots is termed as  $Taifs_m$ . Once the counter is resumed, it is decreased by 1 upon sensing that the channel is idle during one slot. When the backoff counter reaches zero, the corresponding AC starts a transmission if the queue is not empty; otherwise, it continues to wait until receiving a packet. However, if an internal collision occurs, which means that more than one AC finishes the backoff procedure within a station at the same time, the AC with a lower priority fails to access the channel and must repeat the backoff procedure with an enlarged contention window. There are  $M_m + f_m$  backoff stages available prior to dropping a packet of  $AC_m$ , but the contention-window size grows to  $CW_{max_m}$  at stage  $M_m$ . The size of contention window  $CW_{m,i}$  for  $AC_m$  in the  $i$ th backoff stage is given by

$$CW_{m,i} = \begin{cases} 2^i (CW_{min_m} + 1) - 1, & 0 \leq i \leq M_m \\ 2^{M_m} (CW_{min_m} + 1) - 1, & M_m < i \leq M_m + f_m \end{cases} \quad (1)$$

Fig. 3 reveals the timing relation as the described above, in which the successive idle slots are divided into four contention zones corresponding to the number of ACs. Apparently, driven by the default EDCA parameters,  $AC_3$  undoubtedly already finishes the backoff process and waits for the arrival of new packets if the

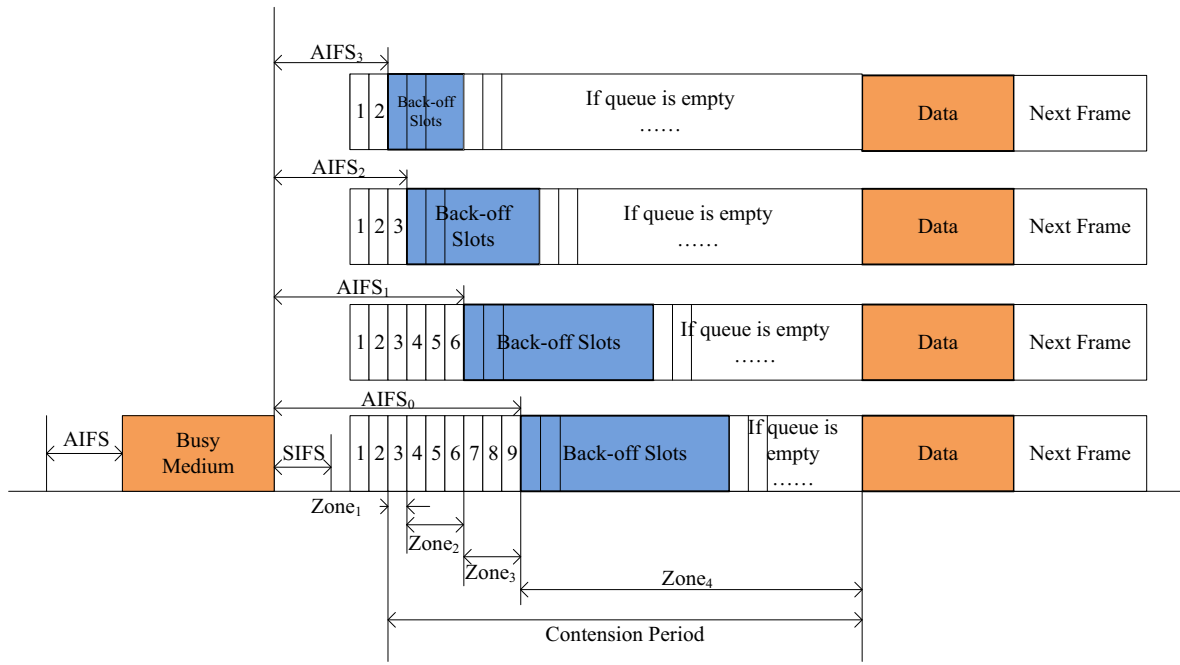


Fig. 3. EDCA timing relation.

channel enters Zone 3 or 4. This implies that the transmission probability of AC<sub>3</sub> in Zones 3 and 4 equals the packet arrival probability within a backoff slot, which obviously differs from the transmission probability in Zones 1 and 2. Therefore, we should use a varying conditional probability instead of a constant to represent the transmission probability for the condition that the channel stays idle for some slots.

To capture the characteristics of an IEEE 802.11p broadcast, we construct a 2-D Markov chain to identify the backoff procedure of AC<sub>m</sub> and establish the relations among all conditional transmission probabilities of ACs. Next, we build a 1-D infinite discrete-time Markov chain to describe the contention period and

establish another relation between the transmission probabilities and the channel state.

### 3.1.1. 2-D Markov chain for the backoff procedure within an AC queue

Fig. 4 represents the dynamic behavior of the EDCA backoff process for AC<sub>m</sub> by using the 2-D Markov chain, in which we use a pair of integers  $(i, j)$  ( $i \in [0, M_m + f_m]$ ,  $j \in [0, W_{m,i} - 1]$ ) to denote the state of the backoff stage and the backoff counter when the queue is not empty, and  $W_{m,i}$  refers to the number of possible backoff counters at stage  $i$  and is expressed by

$$W_{m,i} = CW_{m,i+1} + 1, 0 \leq i \leq M_m + f_m \quad (2)$$

Regarding the empty queue, the state is denoted by  $(0, j)$ ,  $j \in [0, W_{0,i} - 1]$ . The backoff stage for state  $(0, j)$  is called the proactive backoff stage. Accordingly, the probability  $P_m[(i, j)|(k, l)]$  of a one-step transition from state  $(k, l)$  to state  $(i, j)$  within a backoff slot is given by

$$\left\{ \begin{array}{ll} P_m[(0, 0)|(0, 0)] = Pe_m & (3a) \\ P_m[(0, j)|(0, j+1)] = Pe_m, & 0 \leq j \leq W_{m,0} - 2 & (3b) \\ P_m[(0, j)|(0, j+1)] = 1 - Pe_m, & 0 \leq j \leq W_{m,0} - 2 & (3c) \\ P_m[(i, j)|(i, j+1)] = 1, & 0 \leq i \leq M_m + f_m, 0 \leq j \leq W_{m,i} - 2 & (3d) \\ P_m[(1, j)|(0, 0)] = \frac{P_{Cm}(1 - Pe_m)}{W_{m,1}}, & 0 \leq j \leq W_{m,1} - 1 & (3e) \\ P_m[(i, j)|(i-1, 0)] = P_{Cm}/W_{m,i}, & 1 \leq i \leq M_m + f_m - 1, 0 \leq j \leq W_{m,i} - 1 & (3f) \\ P_m[(0, j)|(0, 0)] = \frac{(1 - P_{Cm})(1 - Pe_m)PO_m}{W_{m,0}}, & 0 \leq j \leq W_{m,0} - 1 & (3g) \\ P_m[(0, j)|(i, 0)] = \frac{(1 - Pe_m)PO_m}{W_{m,0}}, & 0 \leq i \leq M_m + f_m - 1, 0 \leq j \leq W_{m,i} - 1 & (3h) \\ P_m[(0, j)|(M_m + f_m, 0)] = PO_m/W_{m,0}, & 0 \leq j \leq W_{m,M_m+f_m} - 1 & (3i) \\ P_m[(0, j)|(0, 0)] = \frac{(1 - P_{Cm})(1 - Pe_m)(1 - PO_m)}{W_{m,0}}, & 0 \leq j \leq W_{m,0} - 1 & (3j) \\ P_m[(0, j)|(i, 0)] = \frac{(1 - P_{Cm})(1 - PO_m)}{W_{m,0}}, & 0 \leq i \leq M_m + f_m - 1, 0 \leq j \leq W_{m,i} - 1 & (3k) \\ P_m[(0, j)|(M_m + f_m, 0)] = (1 - PO_m)/W_{m,0}, & 0 \leq j \leq W_{m,M_m+f_m} - 1 & (3l) \end{array} \right. \quad (3)$$

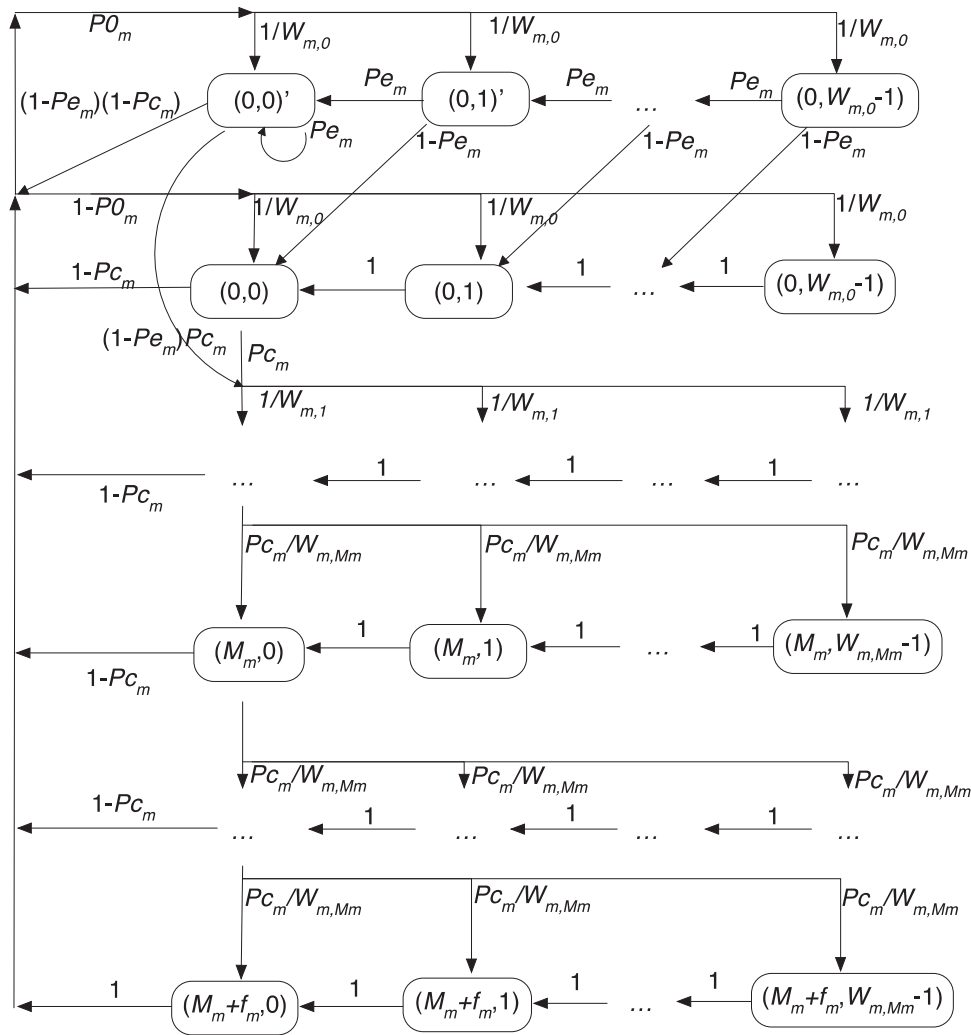


Fig. 4. Markov chain for the backoff procedure.

where  $P_{cm}$  is the average collision probability,  $P_{em}$  is the probability of no packets arriving at the queue within a backoff slot, and  $P_{0m}$  is the probability of the queue becoming empty after a transmission. Eqs. (3a–3c) reflect the case whether or not there are packets arriving after one backoff slot in the proactive backoff stage. Eq. (3d) indicates that the backoff counter is decreased by 1 after one backoff slot. Eqs. (3e) and (3f) explain that the backoff stage is increased by 1 because of the internal collision. Eqs. (3g) and (3i) denote that a new backoff procedure is initiated at the proactive backoff stage if the queue becomes empty after the preceding transmission. Eqs. (3j) and (3l) refer to the case in which the queue is not empty after a transmission. Thus, the stationary probability  $b_{m, i, j}$  of state  $(i, j)$  for AC<sub>m</sub> and the stationary probability  $b'_{m, i, j}$  of state  $(i, j)'$  are expressed by

$$b'_{m,0,0} = F_m \frac{P_{0m}(1-P_{em}^{W_{m,0}})}{W_{m,0}(1-P_{em})^2} \quad (4a)$$

$$b'_{m,0,j} = F_m \frac{P_{0m}(1-P_{em}^{W_{m,0}-j})}{W_{m,0}(1-P_{em})} \quad 1 \leq j \leq W_{m,0} - 1 \quad (4b)$$

$$b_{m,0,j} = F_m \left[ \frac{(W_{m,0}-j)}{W_{m,0}} - \frac{P_{0m}(1-P_{em}^{W_{m,0}-j})}{W_{m,0}(1-P_{em})} \right] \quad 0 \leq j \leq W_{m,0} - 1 \quad (4c)$$

$$b_{m,i,j} = F_m \frac{P_{cm}^i (W_{m,i}-j)}{W_{m,i}} \quad \begin{matrix} 1 \leq i \leq M_m + f_m, \\ 0 \leq j \leq W_{m,0} - 1 \end{matrix} \quad (4d)$$

$$\sum_{j=0}^{W_{m,0}-1} b'_{m,0,j} + \sum_{i=0}^{M_m+f_m} \sum_{j=0}^{W_{m,i}-1} b_{m,i,j} = 1 \quad (4e)$$

where  $F_m$  is the probability that a backoff process finishes (sending or dropping). By solving the Markov chain,  $F_m$  can be derived as

$$F_m = \left[ \sum_{i=0}^{M_m+f_m} \frac{(W_{m,i}+1)}{2} P_{cm}^i + \frac{P_{em}P_{0m}(1-P_{em}^{W_{m,0}})}{W_{m,0}(1-P_{em})^2} \right]^{-1} \quad (5)$$

According to the 2-D Markov chain, for an arbitrary slot, the transmission probability  $\tau_m$  can be calculated through the ratio of the sum of the probabilities of the states with the backoff counter equaling 0 to the sum of the probabilities of all states, as expressed by

$$\tau_m = \frac{b'_{m,0,0}(1-P_{em}) + \sum_{i=0}^{M_m+f_m} b_{m,i,0}}{\sum_{j=0}^{W_{m,0}-1} b'_{m,0,j} + \sum_{i=0}^{M_m+f_m} \sum_{j=0}^{W_{m,i}-1} b_{m,i,j}} (1 - P_{cm}) \quad (6)$$

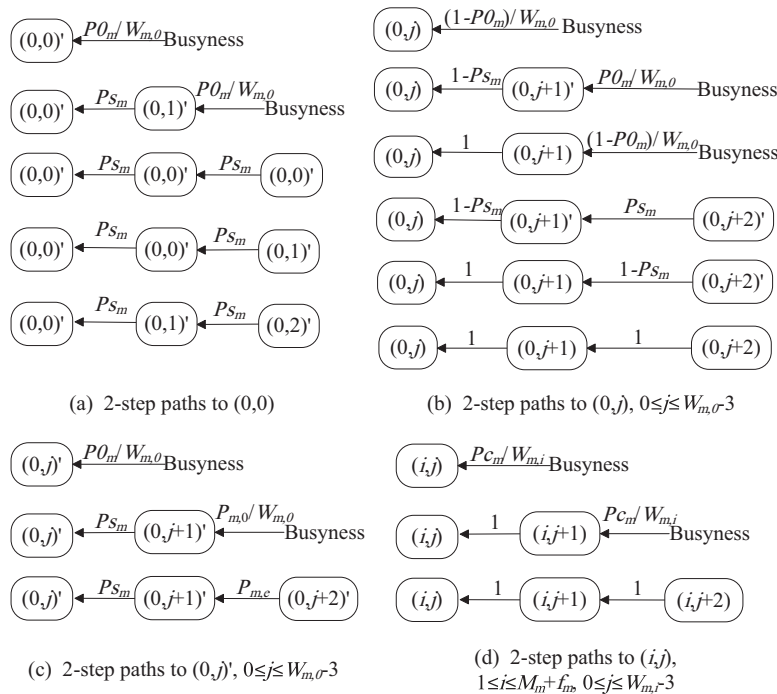


Fig. 5. The paths to state (i, j) within 2 steps.

Eq. (6) covers only the stationary probabilities of the states but is independent of the paths to these states. However, in fact, if the channel has been idle for no fewer than  $k$  slots after the AIFS<sub>m</sub> period, paths in which the channel has become busy in the past  $k$  slots should be excluded from the calculation of the conditional transmission probability. In this case, only the first slot should be the arbitrary slot, for which the probability of a state can be equivalent to its stationary probability. For a clear explanation, we show the paths to state (i, j) by the exact 2 steps in a same backoff stage and the paths within 2 steps starting at the busy state, as shown in Fig. 5.

In Fig. 5,  $P_{s_m}$  refers to the probability of no packets arriving at the queue within an idle slot. Obviously, the paths involving the busy state are impossible if the channel has been 2-slot idle and should be excluded from the probability of state (i, j). Note that an internal collision also indicates busyness because the AC with the highest priority in the collision is able to access the channel.

According to Fig. 5, the probability  $b_{m, i, j, k}$  of state (i, j) for AC<sub>m</sub> that the channel has been  $k$ -slot idle at least after the AIFS<sub>m</sub> period and  $b'_{m, 0, j, k}$  for state (0, j)' are expressed by

$$\begin{cases}
 b'_{m,0,0,k} = \sum_{j=0}^k b'_{m,0,j} P_{s_m}^k & (7a) \\
 b'_{m,0,j,k} = b'_{m,0,j+k} P_{s_m}^k & 1 \leq j \leq W_{m,0} - 1, 0 \leq k & (7b) \\
 b_{m,0,j,k} = b'_{m,0,j+k} \sum_{l=1}^k P_{s_m}^{k-l} (1 - P_{m,s}) + b_{m,0,j+k} & 1 \leq j \leq W_{m,0} - 1, 0 \leq k & (7c) \\
 b_{m,i,j,k} = b_{m,i,j+k} & \begin{matrix} 1 \leq i \leq M_m + f_m, \\ 1 \leq j \leq W_{m,0} - 1, 0 \leq k \end{matrix} & (7d)
 \end{cases}$$

Because the unsaturated condition is covered, the value of  $k$  may be too large, causing the index of  $b_{m, i, j}$  to be out of range. For convenient expression, we define

$$b_{m,i,j} = 0, \quad j > W_{m,i} - 1 \quad (8)$$

Therefore, the transmission probability  $\tau_{m, k}$  that the channel has been  $k$ -slot idle at least after the AIFS<sub>m</sub> period could be expressed by

$$\tau_{m,k} = \frac{b'_{m,0,0,k} (1 - P_{e_{m,k}}) + \sum_{i=0}^{M_m+f_m} b_{m,i,0,k}}{\sum_{j=0}^{W_{m,0}-1} b'_{m,0,j,k} + \sum_{i=0}^{M_m+f_m} \sum_{j=0}^{W_{m,i}-1} b_{m,i,j,k}} (1 - P_{C_m}), \quad k \in [0, +\infty) \quad (9)$$

where  $P_{e_{m, k}}$  is the probability of no packets arriving within the last backoff slot. When  $k=0$ ,  $P_{e_{m, k}}$  equals the probability  $P_{e_m}$  of no packets arriving within an average backoff slot. When  $k > 0$ ,  $P_{e_{m, k}}$  is treated as the probability  $P_{s_m}$  that no packets arrive within a physical slot.

Several notes are given as follows: (i) comparing Eqs. (6) and (9), it can be inferred that the transmission probability within an arbitrary slot is only a special case of the conditional probability  $\tau_{m, k}$ ,  $k=0$ , and (ii) when the value of  $k$  exceeds the maximum of the available contention window sizes,  $\tau_{m, k}$  depends only on

the arrival rate of packets, which is in accordance to the aforementioned analysis.

Furthermore, when AC<sub>m</sub> is allowed to access the channel, the AC<sub>x</sub> with a high priority should experience AIFS<sub>m</sub>-AIFS<sub>x</sub> idle slots at least after its AIFS period, so the internal collision probability

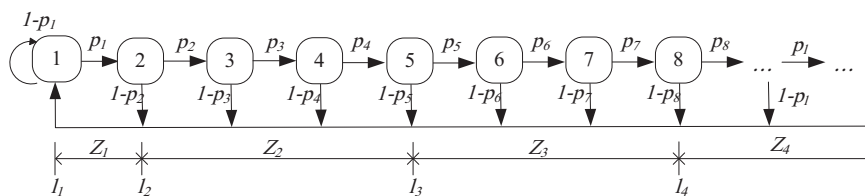


Fig. 6. Markov chain for the contention period.

$PC_m$  can be calculated by

$$PC_m = 1 - \prod_{l=m+1}^3 (1 - \tau_{m,AIFSN_m-AIFSN_x}) \quad (10)$$

### 3.1.2. 1-D Markov chain for the contention period

Fig. 6 constructs a 1-D infinite discrete-time Markov chain to indicate the states of the channel in the contention period, where we use an integer  $l$  to denote the state where the channel comes to the  $l$ th continuous idle slot after entering the contention period. All states are divided into 4 contention zones termed by  $Z_x$  ( $x \in [1,4]$ ), and in  $Z_x$ , there are  $x$  ACs contending for the channel in the priority order. Because the contention period starts with state 1 in the chain, the index  $l_x$  of the initial state of  $Z_x$  can be calculated by

$$l_x = AIFSN_{4-x} - AIFSN_3 + 1 \quad (11)$$

We use  $p_l$  to denote the probability that the channel is idle in state  $l$ , which is expressed by

$$p_l = \prod_{m=4-x}^3 (1 - \theta_{m,l-l_{4-m}})^{N_m}, \quad l \in [1, +\infty), \quad x = \max\{x | l_x < l\} \quad (12)$$

where  $N_m$  is the total number of stations incapable of sending the  $AC_m$  packets, and  $\theta_{m,k}$  is the transmission probability at the  $k$ th continuous idle slot exactly after the  $AIFSN_m$  period; i.e., the channel has been  $l = k + l_{4-m}$ -slot idle since state 0.

The stationary probability  $c_l$  of state  $l$  is expressed by

$$\begin{cases} c_l = c_1 \prod_{i=1}^{l-1} p_i, & l \in [2, +\infty) \quad (13a) \\ \sum_{l=1}^{+\infty} c_l = 1 \quad (13b) \end{cases} \quad (13)$$

We can then derive the relation between  $\theta_{m,k}$  and  $\tau_{m,k}$  as

$$\begin{aligned} \tau_{m,k} &= \frac{\sum_{l=k+l_{4-m}}^{+\infty} \theta_{m,k} c_l}{\sum_{i=k+l_{4-m}}^{+\infty} c_i} \\ &= \theta_{m,k+1} \frac{c_{k+l_{4-m}}}{1 - \sum_{l=0}^{k+l_{4-m}-1} c_l} + \tau_{m,k+1} \frac{1 - \sum_{l=0}^{k+l_{4-m}} c_l}{1 - \sum_{l=0}^{k+l_{4-m}-1} c_l} \quad k \in [0, +\infty) \end{aligned} \quad (14)$$

### 3.2. Access delay affected by channel switching

The access delay is defined as the time interval from a packet reaching the head of the transmission queue until winning the contention and being ready for transmission or until being discarded for exceeding the allowable maximum backoff stage. Considering the immediate state transition upon packet arrival, we ignore the access delay in the proactive backoff stage.

According to the 2-D Markov chain, the average access delay  $ETd_m$  regardless of the channel switching can be derived as

$$ETd_m = \left[ \sum_{i=0}^{M_m+f_m} PC_m \frac{i W_{i+1}}{2} + \frac{P_{0,m}(P_{e,m}-P_{e,m}^{W_{m,0}})}{W_{m,0}(1-P_{e,m})^2} - \frac{P_{0,m}}{(1-P_{e,m})} \right] \times ETs_m \quad (15)$$

where  $ETs_m$  is the average duration of a backoff slot—i.e., the time interval between two successive decrements of the counter. The sum of the two items in the bracket represents the total number of backoff slots over the entire backoff process, and the third indicates the number of backoff slots when the queue is empty, which should be excluded from counting the backoff time.

During the backoff process, an AC enters the frozen state upon sensing that the channel is busy. Concretely speaking, the AC must suspend the backoff counter until the channel recovers and maintains  $AIFS$ -idle interval again. Thus, the probability  $Pf_m$  of  $AC_m$  being frozen and the average duration  $ETf_m$  of the frozen period are expressed by

$$Pf_m = \frac{\sum_{l=l_{4-m}}^{+\infty} c_l (1-p_l)}{\sum_{l=l_{4-m}}^{+\infty} c_l} = \frac{c_{l_{4-m}}}{1 - \sum_{l=0}^{l_{4-m}-1} c_l} \quad (16)$$

$$ETf_m = \frac{Tc_m}{\prod_{l=0}^{l_{4-m}-1} p_l} \quad (17)$$

where  $Tc_m$  is the busy duration sensed for  $AC_m$ , as expressed by

$$Tc_m = Tl + Tairf_s_m + \delta/\sigma \quad (18)$$

where  $Tl$  is the constant spent time of a frame for all ACs including payload, MAC header, and physical header, and  $\delta$  is the propagation delay.

Thus, we can calculate the average duration of a backoff slot as

$$ETs_m = (1 - Pf_m)\sigma + Pf_m ETf_m \quad (19)$$

Let us now consider the impacts of channel switching. We assume that the backoff process of  $AC_m$  starts in a random slot. If the beginning of the backoff process closely approaches the end of the remaining channel time, then it possibly misses the current channel time. Consequently, it must continue in the next synchronization interval, which significantly worsens the entire access delay. To evaluate the impact of this delay, we propose to analyze the transmission over CCH as an example, which is suitable for SCH as well.

For the backoff process spanning  $k$  synchronization intervals on CCH, the synchronization interval is divided into valid and invalid parts. The invalid part refers to the time interval during which the backoff counter is frozen, which includes  $k$  SCH intervals,  $k$  guard intervals, and a remaining  $Tl$  that is too short to accommodate the transmission prior to the channel switching. The durations of the CCH, SCH, guard and synchronization intervals in the slots are termed by  $T_{cch}$ ,  $T_{sch}$ ,  $T_{grd}$  and  $T_{si}$ , respectively. The valid channel duration in  $k$  synchronization intervals for  $AC_m$  is then  $Tu_{m,k} = k \cdot (T_{cch} - T_{grd}) - Tl_m$ . Thus, the probability that the contention starting in a given CCH interval is finished within the  $k$ th CCH,  $k = \lfloor (ETd_m + Tl)/(T_{cch}-T_{grd}) \rfloor$ , is expressed by

$$Pd_m = \frac{Tu_{m,k+1} - ETd_m}{T_{cch} - T_{grd}} \quad (20)$$

Accordingly, for the packets becoming the head of the transmission queue in the valid part of the synchronization interval, we can calculate the average access delay  $ETd_{c_m}$  as

$$ETd_{c_m} = ETd_m + (k + 1 - Pd_m)(T_{sch} + T_{grd})$$

$$= ETd_m \left( \frac{T_{si}}{T_{cch} - T_{grd}} \right) \quad (21)$$

However, if a packet reaches the head of the queue in the invalid channel interval, the duration from that moment to the start of the next CCH interval should be additionally included in the access delay. From the view of the whole network, the time at which the packet arrives in a synchronization interval can be considered uniform. The access delay  $ETds_m$  in which packets become the head of the queue in the invalid interval can then be calculated as

$$ETds_m = ETd_{c_m} + \frac{T_{sch} + T_{grd} + Tl_m}{2} \quad (22)$$

The case in which a packet reaches the head of the queue within the invalid channel interval occurs only when packets enter the transmission queue in the invalid interval and the queue is empty. The average access delay  $ETde_m$  affected by the channel switching is then expressed by

$$ETde_m = \frac{T_{sch} + T_{grd} + Tl_m}{T_{si}} PO_m ETds_m$$

$$+ \left( 1 - \frac{T_{sch} + T_{grd} + Tl_m}{T_{si}} PO_m \right) ETd_{c_m} \quad (23)$$

### 3.3. Solution of the model

To solve the model, we still require the expressions of  $Ps_m$ ,  $Pe_m$  and  $PO_m$ . Because the packet arrival is assumed to follow a Poisson process with rate  $\lambda_m$ , the probability that no packets arrive within a physical slot and a backoff slot can be obtained, respectively, by

$$Ps_m = \exp(-\lambda_m \sigma) \quad (24)$$

$$Pe_m = \exp(-\lambda_m ETs_m) \quad (25)$$

The transmission queue of  $AC_m$  is characterized by an  $M/G/1$  queuing system, in which the arrival rate is  $\lambda_m$  and the mean value of the service time is  $ETde_m$ . Thus, the probability of an empty queue is expressed by

$$PO_m = 1 - \lambda_m ETde_m \quad (26)$$

where  $ETde_m$  is already expressed by  $PO_m$  in Eqs. (15) and (21), so  $PO_m$  can be solved using an expression of  $ETs_m$  according to Eqs. (15), (21) and (24), as expressed by

$$PO_m = \left( 1 - \lambda_m ETs_m \sum_{i=0}^{M_m + f_m} P_{C_m}^i \frac{W_i + 1}{2} \right) \left( \frac{T_{si}}{T_{cch} - T_{grd}} \right) / \Gamma \quad (27)$$

$$\Gamma = 1 + \lambda_m \left\{ ETs_m \left[ \frac{(Pe_m - Pe_m^{W_{m,0}})}{W_{m,0}(1 - Pe_m)^2} - \frac{1}{(1 - Pe_m)} \right] \left( \frac{T_{si}}{T_{cch} - T_{grd}} \right) \right.$$

$$\left. + \frac{(T_{sch} + T_{grd} + Tl_m)^2}{2T_{si}} \right\} \quad (28)$$

$$\left\{ \begin{array}{l} P_{n_{m,k}} = \prod_{i=4-x}^3 (1 - \theta_{i,k})^{N_i - 1}, \quad 0 \leq k < l_{\max} - l_{4-m}, \\ P_{n_{m,l_{\max} - l_{4-m}}} = \prod_{i=0}^3 (1 - \tau_{i,l_{\max} - l_{4-i}})^{N_i - 1}, \quad x = \max\{x | l_x \leq k + l_{4-m}\} \end{array} \right. \quad (31a)$$

$$\left\{ \begin{array}{l} P_{n_{m,k}} = \prod_{i=4-x}^3 (1 - \theta_{i,k})^{N_i - 1}, \quad 0 \leq k < l_{\max} - l_{4-m}, \\ P_{n_{m,l_{\max} - l_{4-m}}} = \prod_{i=0}^3 (1 - \tau_{i,l_{\max} - l_{4-i}})^{N_i - 1}, \quad x = \max\{x | l_x \leq k + l_{4-m}\} \end{array} \right. \quad (31b)$$

At this point, enough relations have been found to solve the proposed models. Starting with the probability of state 1 in the 1-

D Markov chain in Fig. 6, all variables of each AC can be expressed by the order of the continuous idle slots. To be specific, by knowing the probability  $c_1$ , the packet arrival rate, and the standard parameters, we can calculate the others as follows.

- Step i. Set  $l = 1$  and  $m = 3$ ;
- Step ii. Set  $l' = l_{4-m}$ ;
- Step iii. Calculate  $ETs_m$  using Eqs. (16), (17), (18) and (19);
- Step iv. Calculate  $Pe_m$  and  $PO_m$  using Eqs. (25) and (27), respectively;
- Step v. Calculate  $\tau_{m,k}$  using Eqs. (7) and (9),  $k \in [0, +\infty)$ ;
- Step vi. Calculate  $P_{C_{m-1}}$  using Eq. (10) if  $m > 0$ ;
- Step vii. Calculate  $\theta_{m,l-l'}$  using Eq. (14);
- Step viii. Calculate  $p_l$  using Eq. (12);
- Step ix. Calculate  $c_{l+1}$  using Eq. (13a), and set  $l = l + 1$ ;
- Step x. Loop steps vii–ix until  $l = l_{4-m+1}$  or  $l = l_{\max}$ ;
- Step xi. If  $l = l_{\max}$ , then exit; otherwise, set  $m = m - 1$  and go to step ii.

Herein, the probabilities of all states in the 1-D Markov chain are expressed in the form of  $c_1$ , and regarding the constraint of Eq. (13b), the probability  $c_1$  can be solved. One note is that the theoretical value of  $l_{\max}$  is infinite; however, we set  $l_{\max} = l_4 + 1$  in the calculations as a compromise between accuracy and complexity. In the cases of  $l > l_4 + 1$ , we substitute the average probability  $\tau_{m,l_4+1-l_{4-m}}$  for all  $\theta_{m,l-l_{4-m}}$ .

Next, we can calculate the performance metrics—e.g., the access delay and the packet delivery rate (PDR). The access delay can be obtained directly by Eq. (23). The PDR is defined as the ratio of the number of packets successfully received to the total number of packets. Because the channel switches every 50 ms, the PDR is affected significantly by the synchronization of the transmission at the beginning of the valid channel interval. Packets entering the queues within the invalid interval will be transmitted simultaneously if the AC queues are empty and their backoff counters are 0 at that moment—i.e., the ACs are in state (0, 0)'. Thus, we calculate the PDR regarding two situations—i.e., synchronized packet delivery rate  $PDR_s$  and ordinary packet delivery rate  $PDR_o$ :

$$PDR_m = \frac{T_{cch} - T_{grd}}{T_{si}} b'_{m,0,0} PDR_s$$

$$+ \left( 1 - \frac{T_{cch} - T_{grd}}{T_{si}} b'_{m,0,0} \right) PDR_o \quad (29)$$

The synchronized packet delivery rate  $PDR_s$  equals the probability that the ACs of other stations with the same priority in (0, 0)' fail to receive a packet from the upper level within an invalid interval, and the ACs with higher priority have no packets to transmit. Thus, it can be expressed by

$$PDR_s = \{ 1 - \exp[-\lambda_m (T_{sch} + T_{grd} + Tl_m)] \}^{(N_m - 1) b'_{m,0,0}}$$

$$\times \prod_{i=4-m}^3 (1 - \theta_{i,k})^{N_i - 1} \quad (30)$$

Considering the ordinary packet delivery rate, because only one AC queue can send a packet at any time, the probability  $Pn_{m,k}$  of only the current node's  $AC_m$  transmitting in the corresponding contention zones can be calculated by

$$Ch_{m,k} = \frac{c_{k+l_{4-m}} \theta_{m,k}}{\tau_{m,0} \sum_{l=l_{4-m}}^{l_{\max}} c_l}, \quad 0 \leq k < l_{\max} - l_{4-m} \quad (31)$$

In addition, by Bayes' theorem, the probability of the transmission occurring at the  $k$ th slot after the AIFS<sub>m</sub> period is expressed by

$$Ch_{m,k} = \frac{c_{k+l_{4-m}} \theta_{m,k}}{\tau_{m,0} \sum_{l=l_{4-m}}^{l_{\max}} c_l}, \quad 0 \leq k < l_{\max} - l_{4-m} \quad (32)$$

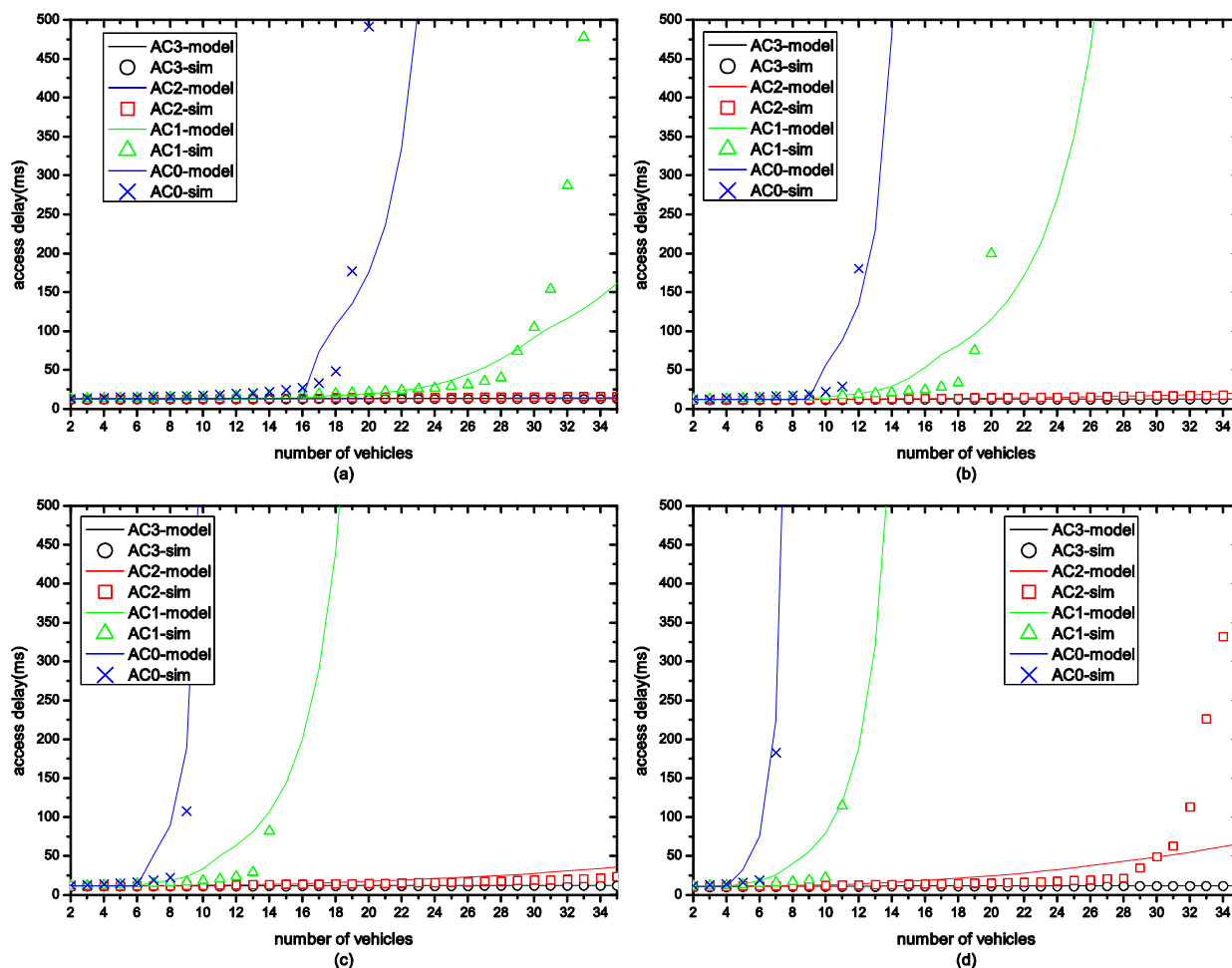


Fig. 7. Access delay vs. number of vehicles. (a)  $\lambda_0 = \lambda_1 = \lambda_2 = \lambda_3 = 15$ , (b)  $\lambda_0 = \lambda_1 = \lambda_2 = \lambda_3 = 20$ , (c)  $\lambda_0 = \lambda_1 = \lambda_2 = \lambda_3 = 25$ , and (d)  $\lambda_0 = \lambda_1 = \lambda_2 = \lambda_3 = 30$ .

Thus,  $PDR_o$  of  $AC_m$  corresponds to the average value, as expressed by

$$PDR_o_m = \sum_{k=0}^{l_{\max} - l_{4-m}} Ch_{m,k} Pn_{m,k} \quad (33)$$

#### 4. Numerical results

In this section, we verify the effectiveness of the performance model derived in Section 3 through simulation results. The simulations were conducted using network simulator 3.24 (NS3.24). Each simulation lasts for 200 s. We focus on a network scenario with  $N$  vehicles in a single contention domain. All  $N$  vehicles have one single-radio WAVE device operating in an alternative-switching mode with two IEEE 802.11p MAC entities for CCH and SCH, and they can transmit packets with all four ACs—i.e.,  $N_0 = N_1 = N_2 = N_3 = N$ . The data packets arrive at the  $AC_m$  queue following a Poisson process with mean  $\lambda_m$ . We use the PDR and the average access delay underlying the MAC layer as the relevant performance indicators. Compared with the throughput and the end-to-end delay, the focused PDR and the average access delay are considerably more significant for the broadcast service because there is no retransmission to ensure that the packets are received correctly. We extensively investigate the performance metrics against various combinations of packet arrival rates and numbers of vehicles in a single contention domain. We use the default

Table 2

Parameter values.

Parameter	Value
$aCW_{min}$	15
$aCW_{max}$	1023
Frame payload	4096 bits
MAC header	88 bits
Bit rate	6 Mbps
PLCP Preamble	32 $\mu$ s
PLCP Signal	8 $\mu$ s
SIFS	32 $\mu$ s
Physical slot ( $\sigma$ )	13 $\mu$ s
Propagation delay ( $\delta$ )	1 $\mu$ s

values of the EDCA parameters  $CW_{min}$ ,  $CW_{max}$  and  $AIFS_N$  defined by IEEE 802.11p, as shown in Table 1. The default values of multichannel operation parameters CCH, SCH, guard and synchronization interval are defined by IEEE 1609.4, and the other parameters in the simulation experiments are given in Table 2.

Fig. 7 shows the access delay of each AC against different numbers of vehicles, where the access delay deteriorates with increasing number of vehicles. It is observed that the analytical results fit the simulation results well, which means that the analytical model is accurate and effective. When the number increases beyond a threshold value for an AC (e.g.,  $N = 12$  for  $AC_0$  in Fig. 7b), the access delay increases dramatically. Meanwhile, the threshold value

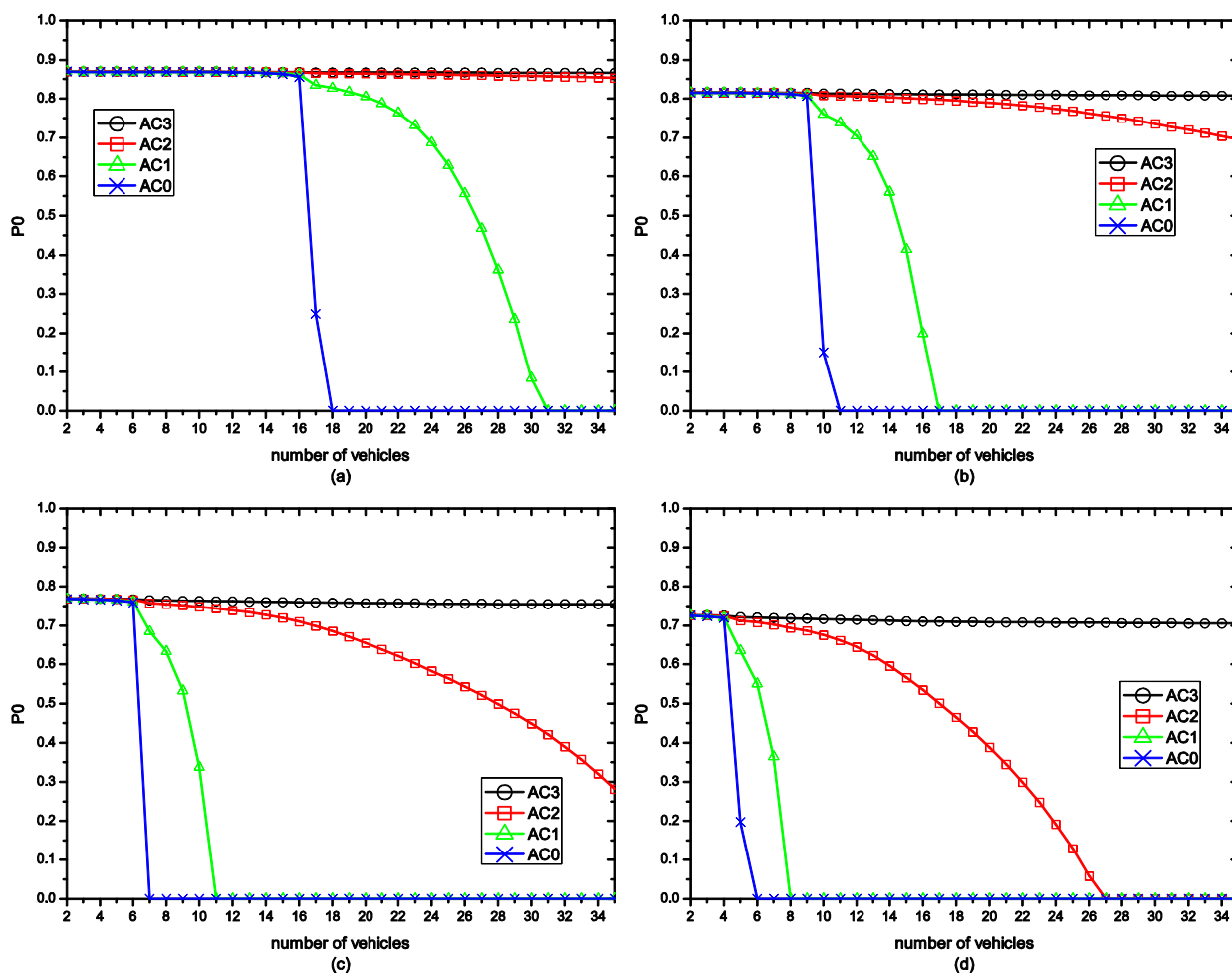


Fig. 8.  $P_0$  vs. the number of vehicles. (a)  $\lambda_0 = \lambda_1 = \lambda_2 = \lambda_3 = 15$ , (b)  $\lambda_0 = \lambda_1 = \lambda_2 = \lambda_3 = 20$ , (c)  $\lambda_0 = \lambda_1 = \lambda_2 = \lambda_3 = 25$ , and (d)  $\lambda_0 = \lambda_1 = \lambda_2 = \lambda_3 = 30$ .

shifts left with increasing arrival rate, which is because the duration time of the frozen period plays a key role in the total delay because there is no retransmission, and the duration of the frozen time is determined by the AIFSN and the probability that the channel remains successively idle. As more vehicles join the contention for the channel simultaneously, the probability of the availability of continuous idle slots is sharply reduced, especially for the AC with a large AIFSN. Therefore, apparently, compared with AC<sub>3</sub> and AC<sub>2</sub>, the access delays of AC<sub>0</sub> and AC<sub>1</sub> are considerably more influenced by the number of vehicles.

Fig. 8 shows the probability  $P_0$  of the transmission queue being empty against various numbers of vehicles. It can be inferred that the probabilities  $P_0$  of AC<sub>0</sub> and AC<sub>1</sub> begin to sharply decrease to 0 once the number of vehicles contending for the channel reaches a certain value, which is because the access delay decreases with increasing number of vehicles. When the average access delay exceeds the average interval time between the successive arrivals of packets, the probability that the transmission queue is empty slides down to 0, which means that the AC reaches a saturated state. In contrast, the AC queues with a small AIFSN always behave in a large probability to remain empty because the number of vehicles has little effect on the access delay.

Fig. 9 shows the transmission probability against various numbers of successive idle slots after entering the contention period. It can be observed that for the ACs in the unsaturated condition, such as all ACs in Fig. 9(a), AC<sub>1</sub>–AC<sub>3</sub> in Fig. 9(b), AC<sub>2</sub> and AC<sub>3</sub> in Fig. 9(c)

and Fig. 9(d), the transmission probabilities decrease with increasing number of the continuous idle slots. This is because the transmission queues of these ACs remain empty with high probability, and the packets easily arrive in the frozen period. Thus, the closer the frozen period, the higher the transmission probability. Moreover, because of the longer frozen time duration, the AC with larger AIFSN has a higher transmission probability in the same condition. However, when an AC reaches a saturated condition—e.g., AC<sub>0</sub> in Fig. 9(b)–9(d), and AC<sub>1</sub> in Fig. 9(c) and Fig. 9(d)—the transmission probabilities begin to improve as the number of continuous idle slots increases. This is because the transmission queues of these ACs always have packets to send, and the backoff is bound to be over within the restrictive time. Thus, the closer to the end of the backoff, the higher the transmission probability. In this case, owing to the small size of the contention window, the AC with a small AIFSN has a high transmission probability instead, as shown in Fig. 9. Therefore, we can conclude that the closer the saturation, the greater influence the AC can bring on the PDR of the ACs with a lower priority.

Fig. 10 shows the PDR against various numbers of vehicles. It can be observed that the PDR decreases with increasing number of vehicles because the access delay deteriorates with increasing number of vehicles, and the simulation results are broadly in accordance with the analytical results. However, it can also be observed that the slopes of these curves experience an abrupt change at some points, which causes the curves to accelerate or decelerate.

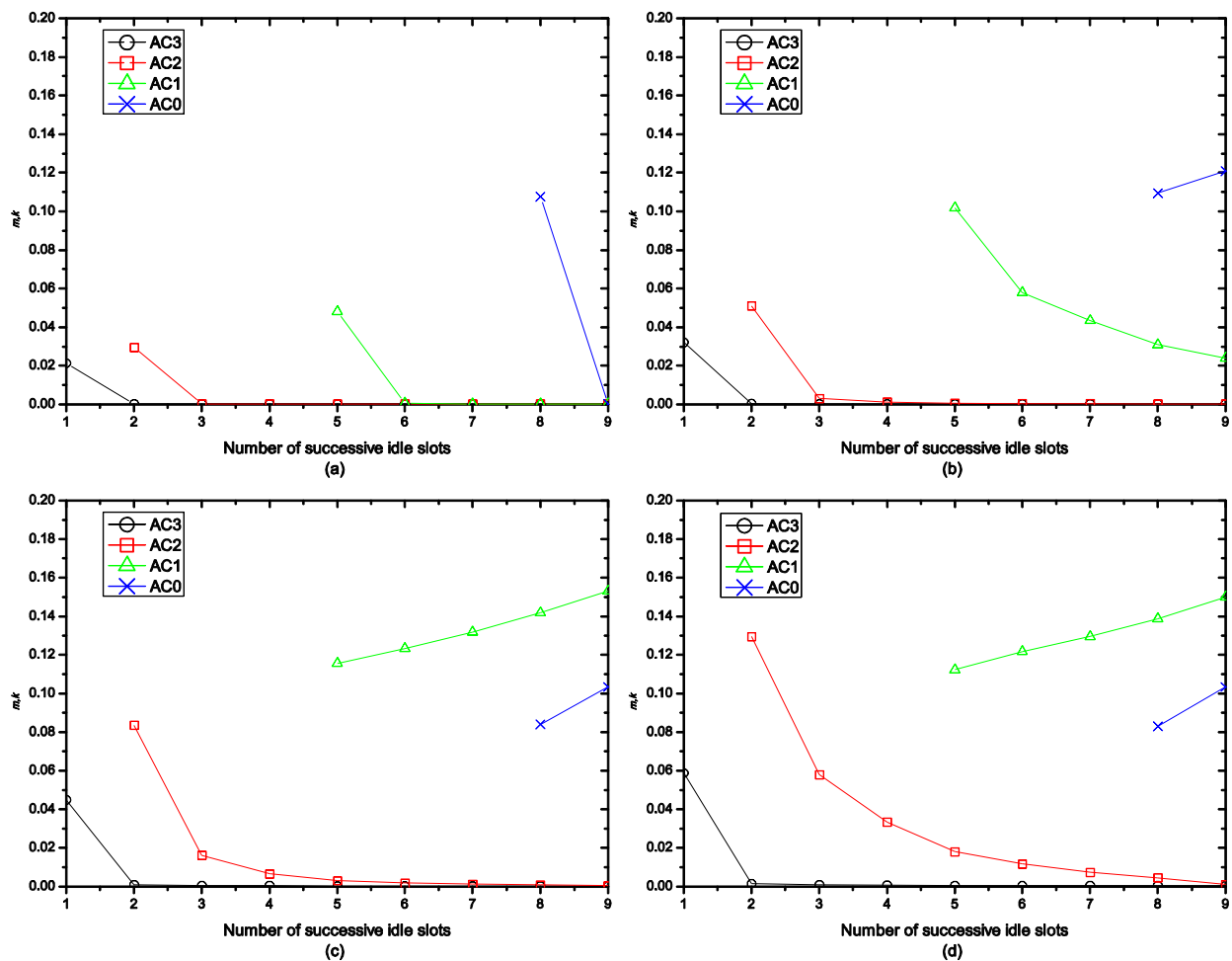


Fig. 9. Transmission probability vs. the number of successive idle slots.  $N=15$ , (a)  $\lambda_0=\lambda_1=\lambda_2=\lambda_3=15$ , (b)  $\lambda_0=\lambda_1=\lambda_2=\lambda_3=20$ , (c)  $\lambda_0=\lambda_1=\lambda_2=\lambda_3=25$ , and (d)  $\lambda_0=\lambda_1=\lambda_2=\lambda_3=30$ .

ate their descent, such as AC<sub>0</sub> at  $N=17$  in Fig. 10(a), AC<sub>0</sub> at  $N=9$  and AC<sub>1</sub> at  $N=10$  in Fig. 10(b), AC<sub>0</sub> at  $N=7$ , AC<sub>1</sub> at  $N=7$  and AC<sub>2</sub> at  $N=7$  in Fig. 10(c), AC<sub>0</sub> at  $N=5$ , AC<sub>1</sub> at  $N=6$ , and AC<sub>2</sub> at  $N=6$  in Fig. 10(d). This is because the PDR is affected by two factors: synchronized packet delivery rate and ordinary packet delivery rate. As the number of vehicles and the packet arrival rate increase, the probability that the transmission queues are empty is decreased—i.e., the impact of the synchronized packet delivery rate is reduced—whereas the synchronized packet delivery rate is much less than the ordinary packet delivery rate. According to the analysis in Fig. 8, it can be inferred that the abrupt change point of the PDR is just the sharp decline point of  $P_0$ , and  $P_0$  declines much sharply, so the PDR changes drastically. In addition, by observing the simulation results, one can know that the ACs with a low priority has better PDRs and that the packet arrival rate is low with a small number of vehicles. There are two reasons for this: (i) according to the analysis in Fig. 9, one can know that the majority of transmissions occur exactly at the first idle slot of their contention zones if the ACs does not reach the saturated condition. There is little interaction effect between different ACs; (ii) the AC with a low priority is less affected by the synchronized packet delivery rate owing to the high access delay and large contention window size. However, the second reason is not perfectly reflected in our model. This is mainly because in the actual proactive backoff stage, because the channel switches every 50 ms, the transition between the states does not always depend on the probability of packets

arriving within a backoff slot, which must be analyzed by a more complicated model. This is the focus of our future work.

## 5. Conclusions

This paper presented a comprehensive model to analyze the performance of a prioritized broadcast service in WAVE/IEEE 802.11p. We investigated two important QoS metrics for the broadcast applications—i.e., the access delay and PDR. The main contributions to the literature are summarized as (i) the transmission probability is not assumed to be a constant, and we deduced the formula of the transmission probability against various numbers of successive idle slots; (ii) we captured the backoff procedure where no packets wait in the queue, which is proved essentially by the analytical results in which the queue is always empty; and (iii) we considered the effects of the periodic CCH/SCH switching on the access delay and PDR, which is the main feature of WAVE. The simulation results faithfully verified that the analytical model is accurate and effective. Our future work will be focused on comprehensively modeling the impacts of the synchronization caused by multichannel operation.

## Acknowledgments

This work was supported by the National Nature Science Foundation [51175215, 61202472, 61373123, 61572229]; the Research

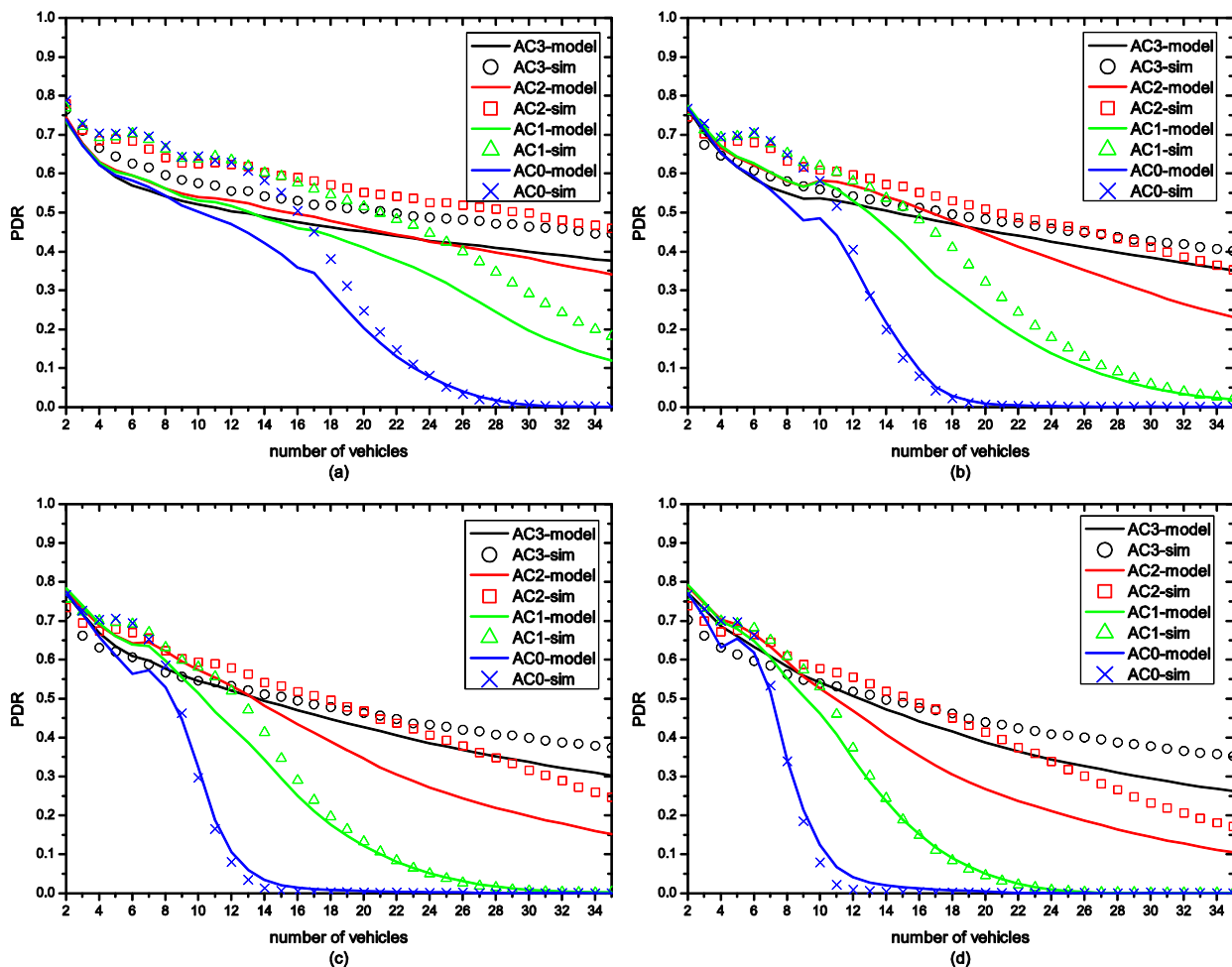
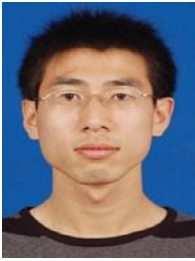


Fig. 10. PDR vs. the number of vehicles. (a)  $\lambda_0 = \lambda_1 = \lambda_2 = \lambda_3 = 15$ , (b)  $\lambda_0 = \lambda_1 = \lambda_2 = \lambda_3 = 20$ , (c)  $\lambda_0 = \lambda_1 = \lambda_2 = \lambda_3 = 25$ , and (d)  $\lambda_0 = \lambda_1 = \lambda_2 = \lambda_3 = 30$ .

Fund for the Doctoral Program of Higher Education of China [20120061120060]; the Scientific Research Foundation for Returned Scholars; the International Scholar Exchange Fellowship (ISEF) program of the Korea Foundation for Advanced Studies (KFAS); the Foundation of State Key Laboratory of Automotive Simulation and Control [20120108]; the Jilin Provincial Foundation for Young Scholars [20130522116JH]; jilin University Young Teacher and Student Cross Discipline Foundation [JCKY-QKJC09]; and the Jilin Provincial International Cooperation Foundation [20140414008GH, 20150414004GH].

## References

- [1] IEEE Computer Society, "IEEE Standard for Information technology - Telecommunications and information exchange between systems - Local and metropolitan area networks Specific requirements, Part 11: Wireless LAN Medium Access Control (MAC) and Physical Layer (PHY) Specifications, Amendment 6: Wireless Access in Vehicular Environments", IEEE Std 802.11p™-2010. IEEE New York USA, July 2010.
- [2] IEEE Vehicular Technology Society, "IEEE Standard for Wireless Access in Vehicular Environments (WAVE) - Multi-channel Operation", IEEE Std 1609.4™-2010, IEEE, New York, USA, February 2011.
- [3] J.R. Gallardo, D. Makrakis, H.T. Mouftah, Performance analysis of the EDCA medium access mechanism over the control channel of an IEEE 802.11p wave vehicular network, in: IEEE International Conference on Communications, 2009, pp. 5063–5068.
- [4] K.A. Hafeez, L. Zhao, Z. Liao, B.N. Ma, Performance analysis of broadcast messages in VANETs safety application, in: 2010 IEEE Global Telecommunications Conference (GLOBECOM 2010), 2010, pp. 1–5.
- [5] W. Rinaru, H.D. Seog, S. Jung-Hoon, Performance analysis for priority based broadcast in vehicular networks, in: International Conference on Ubiquitous and Future Networks, 2013, pp. 51–55.
- [6] P. Wang, F. Wang, Y. Ji, Performance analysis of EDCA with strict priorities broadcast in IEEE802.11p VANETs, in: 2014 International Conference on Computing, Networking and Communications, 2014, pp. 403–407.
- [7] H. Qiu, W.-H. Ho, C.K. Tse, Y. Xie, A methodology for studying 802.11p vanet broadcasting performance with practical vehicle distribution, IEEE Trans. Vehicular Technol. 64 (10) (2014) 4756–4769.
- [8] N. Ferreira, J. Fonseca, On the end-to-end delay analysis for an IEEE 802.11p/WAVE protocol, in: 18th IEEE Symposium on Communications and Vehicular Technology in the Benelux (SCVT), 2011, pp. 1–6.
- [9] C. Han, M. Dianati, R. Tafazolli, R. Kernchen, Analytical study of the IEEE 802.11p MAC sublayer in vehicular networks, IEEE Trans. Intell. Transp. Syst. 13 (2) (2012) 873–886.
- [10] W. Sun, H. Zhang, C. Pan, J. Yang, Analytical study of the IEEE 802.11p EDCA mechanism, in: IEEE Intelligent Vehicles Symposium, 2013, pp. 1428–1433.
- [11] J. Zheng, Q. Wu, Performance modeling and analysis of the IEEE 802.11p EDCA mechanism for VANET, IEEE Trans. Vehicular Technol. 65 (4) (2015) 2673–2687, doi:10.1109/TVT.2015.2425960.
- [12] J. Misić, G. Badawy, V.B. Misić, Performance characterization for IEEE 802.11p network with single channel devices, IEEE Trans. Vehicular Technol. 60 (4) (2011) 1775–1787.
- [13] C. Campolo, A. Molinaro, A. Vinel, Y. Zhang, Modeling event-driven safety messages delivery in IEEE 802.11p/WAVE vehicular networks, IEEE Commun. Lett. 17 (12) (2013) 2392–2395.
- [14] X. Yin, X. Ma, K.S. Trivedi, Performance of BSM dissemination in multi-channel DSRC, in: IEEE 77th Vehicular Technology Conference (VTC Spring), 2013, pp. 1–7.
- [15] F. Kaabi, P. Cataldi, F. Filali, C. Bonnet, Performance analysis of IEEE 802.11p control channel, in: Sixth International Conference on Mobile Ad-hoc and Sensor Networks (MSN), 2010, pp. 211–214.
- [16] C. Claudia, V. Alexey, M. Antonella, Modeling broadcasting in IEEE 802.11p/WAVE vehicular networks, IEEE Commun. Lett. 15 (2) (2011) 199–211.



**Peng Zhou** received his M.S. degree in College of Computer Science and Technology from Jilin University in 2012. He is interested in topics related to vehicular networks, especially for MAC protocols and cross-layer optimization. He is currently studying Computer Application Technology at Jilin University to get his Ph.D. degree.



**Yanheng Liu** received M.Sc. and Ph.D degrees in computer science from Jilin University, People's Republic of China. He is currently a professor in Jilin University, People's Republic of China. His primary research interests are in network security, network management, mobile computing network theory and applications, etc. He has co-authored over 90 research publications in peer reviewed journals and international conference proceedings of which one has won "best paper" awards. Prior to joining Jilin University, he was visiting scholar with University of Hull, England, University of British Columbia, Canada and Alberta University, Canada.



**Jian Wang** received his B.Sc., M.Sc., and Ph.D. degrees in Computer Science from Jilin University, respectively in 2004, 2007, and 2011. He is interested in topics related to wireless communication and vehicular networks, especially for network security and communication modeling. He has published over 40 articles on international journals and conferences. Currently he is an associate professor in Jilin University, and a visiting scholar in Hanyang University, South Korea.



**Weiwen Deng** was a Staff Research in General Motors Global R&D Center. In 2010, he briefly served as Acting Director of Hong Kong APAS R&D Center. Currently, he is a Professor in Jilin University. Also he is the Editor-in-Chief of "International Journal of Vehicle Autonomous Systems", and Associate Editors of "International Journal of Vehicle Design" and "IEEE Transaction on Vehicular Technology".



**Heekuck Oh** received his B.S. degree in Electronics Engineering from Hanyang University in 1983. He received his M.S. and Ph.D. degrees in Computer Science from Iowa State University in 1989 and 1992, respectively. In 1994, he joined the faculty of the Department of Computer Science and Engineering, Hanyang University, where he is currently a professor. His current research interests include network security and cryptography. He is President Emeritus of Korea Institute of Information Security & Cryptology, a member of Advisory Committee for Digital Investigation in Supreme Prosecutors' Office of the Republic of Korea, a member of Advisory Committee on Government Policy, and a member of ISMS PIMS Accreditation Board of Korea.